A new generation SQUID biosusceptometer

T.N. Starr[1], R. Fischer[2,3], T. Ewing[1], F. Longo[3], R. Engelhardt[2], E. Trevisiol[3], R.L. Fagaly[1],
D.N. Paulson[1], and A. Piga[3]

[1]*Tristan Technologies Inc., San Diego, CA 92121, U.S.A.;* [2]*Institut f. Medizinische Biochemie u. Molekularbiologie, Universitaet Hamburg, D-20246 Hamburg, Germany;* [3]*Dipartimento di Scienze e dell' Adolescenza, Università degli Studi di Torino, I-10126 Torino, Italy*

1 Introduction

Iron overload from genetic disorders and/or regular blood transfusions is a serious health problem in many regions of the world. As liver and spleen iron stores account for more than 70 % of total body iron stores, the precise quantification and the continuous monitoring of these stores is of particular importance in the diagnosis and treatment of these disorders. During the last two decades several non-invasive methods have been explored for the assessment of elevated liver iron stores in patients with primary (genetic hemochromatosis) or with iron loading anemias (e.g., ß-thalassemia major, leukemia after bone marrow transplantation). Of these different methods only quantitative magnetic resonance imaging (qMRI) [1] and SQUID biomagnetic liver susceptometry (BLS) [2] have achieved a broader clinical acceptance. The non-invasive determination of liver iron concentration (LIC) by BLS has become now a routine method in iron overload monitoring. While serum ferritin has been shown to be only a poor predictor of iron overload [3, 4] many European thalassemia centers in Italy, Greece, Switzerland and Germany are using BLS now as part of their regular follow-up programme.

From the experience of two decades with SQUID susceptometers [4, 5] we have developed a novel low temperature 3-channel SQUID biosusceptometer system (SQUID BioSusceptometer, model 5700, Tristan) for the Centro Microcitemie at the hospital O.I.R.M. / S. Anna in Turin.

The system was especially optimized for

1. improved spatial resolution: below liver iron concentrations of 1000 µg Fe/g_{liver} and in obese patients, the approximate estimation of the magnetic susceptibility of the thorax tissue layer above the liver was the main limiting factor in the precision of the determination of LIC by SQUID-BLS.
2. pediatric measurements: as many of the patients are children with small sized livers and spleens, certain system components such as the waterbag reference, the sensor assembly and the dewar tail had to be optimized in order to allow measurements in pediatric patients <= 3 years old.
3. clinical practicability: as the quality of the data depend largely on the individual positioning of the subjects, many components, such as laser cross alignment used for positioning and the evacuable patient mattress, had to be integrated into the system.

2 System and Methods

2.1 System components and schematic

The design of the system and the operational procedures are based in part on the experience and the developments made on the biosusceptometer at the university of Hamburg in an area of low environmental magnetic noise [6]. The major physical subsystems of the Torino Biosusceptometer are:

- S*ensor assembly and electronics:* comprised of a 35 mT dc superconducting magnet (1st order gradient-wound coil with radius r = 1.6 cm and baseline d = 12.6 cm) and three different concentric 2nd order gradiometers. A far-field sensitive symmetrical 2nd order gradiometer (channel A), a near-field sensitive planar gradiometer (B), and a small-field sensitive 2nd order gradiometer (C) were optimized for susceptometry in children and adults. The gradiometers are coupled to niobium dc SQUIDs resulting in a sensitivity of 9 nT/V (for channel A). The electronics consists of a 3-channel SQUID control unit (IMC-303, Tristan Tech., U.S.A.) and flux-locked loops (IFL-301-H). The whole assembly is composed from G-10 coil bodies and integrated into the vacuum section inside the 10 cm fiber-glass tail of the dewar. The assembly is configured for minimum cross-talk and optimal spatial resolution.
- *Liquid helium dewar*: a newly designed aluminium dewar (BMD-35M) of minimum

magnetic signature and with a capacity of 35 L allows a maximum standing time of 10 days with at a boil-off rate of < 3.4 L/day for regular liquid helium delivery.

- W*ater reference*: a micro-computer controlled water coupling membrane system has been developed consisting of a small sized bellows system (R = 20 cm), a frequency controlled impeller pump unit, and electric PVC valves of low magnetic signature. The water reservoir has an integrated heating (35 °C).
- *Gantry*: a newly designed wood structure of esthetic appearance is mounted on vibration isolation pads. Along with supporting the dewar and the water coupling membrane system, the gantry takes up internal routing of cabling, water piping and a membrane compressor/pump for the evacuation of the patient mattress.
- *Patient bed*: constructed of an aluminium frame and table tops of honey-comb structure. It allows manual translation in the horizontal x-y directions and motor-controlled vertical movement at max. bed speed of 1 cm/s over a total travel of 30 cm. A vertical bed height position transducer allows relative distance measurements in z direction for rigid phantoms. Moreover, the light-weighted bed can be rolled easily over the floor from the bed-side sonography position to the measurement position beneath the dewar tail.
- *Positioning system:* consists of integrated locator loop circuits as described elsewhere [7] with waveform generator and software generated lock-ins at 3 different frequencies, a cross plane laser (LAP Pc-K, LAP GmbH, Germany) mounted at the ceiling for indicating the sonography position, and an evacuable patient mattress.
- *Active noise cancellation*: performed by a miniature 3-axis fluxgate magnetometer (mod. 534, Applied Physics Systems, U.S.A.) mounted in one of the gantry poles.
- *Process control* (handheld control, water pressure control, patient bed motion, position location), the *data acquisition* (National Instruments DAC cards: PCI-6023E and PCI–6031E) and the *online analysis* is done under Windows 98 and LabWindows CVI (National Instruments) on a 400 MHz PC. SQUID data are taken at a max. sampling rate 100 kS/s.
- *Ultrasound imager*: real-time scanner (Eidos, ESAOTE, Italy) with a large linear probe (3.5 MHz) allows distance and area measurements including ellipsoidal fitting of organ geometries.
- *Auxillary system*: consists of a 2nd workstation for a refined offline analysis under HP Basic for Windows and a 2nd patient bed for separate liver volume measurements by ultrasound or separate pre-positioning of patients.

In Fig. 1, a schematic representation of the major physical subsystems is displayed together with the routing of control and data signals.

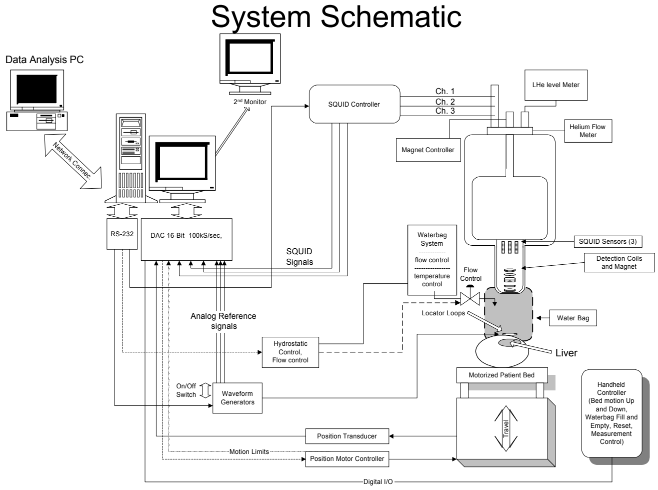

Figure 1: *System schematic of the Torino Biosusceptometer.*

2.2 Methods

Calibration: The analysis of measurements with SQUID biosusceptometers makes use of the reciprocity theorem of susceptometry [8]. From this theorem on magnetic flux integrals f($\mathbf{B}_f$, $\mathbf{B}_d$, $\mathbf{r}$), a linear equation is derived in order to determine the relative magnetic volume susceptibility, $\Delta\chi_{obj} = \chi_{obj} - \chi_{ref}$, of an object or subject versus a reference medium (water, air) from the SQUID data V(z):

$$V(z) = V_o + C_j\Delta\chi_{obj}\int_V (\mathbf{B}_f \cdot \mathbf{B}_d) d^3r + \Delta V_{sys}(z) \quad (1)$$

Before biosusceptometry can be applied to patients, the calibration constants C_j and the system backgrounds ΔV_{sys} (z) for all 3 gradiometer channels have to be determined. The relatively small system background signals resulting from the locator loop and the water coupling membrane (water reference) or from the locator loop only (air reference) are measured on supports with low magnetic signature as function of distance using the bed position transducer.

Active noise cancellation: Postulating the raw signal $\mathbf{V}_{raw}$ in the 3 concentric gradiometer channels to be a linear superposition of the desired signal $\mathbf{V}_{ABC}$ and the environmental noise, one has to subtract this noise signal as measured by the fluxgate reference detector $\mathbf{V}_{XYZ}$ [9]:

$$\mathbf{V}_{ABC} = \mathbf{V}_{raw} - \left(\boldsymbol{\omega}_{jk}\right) \cdot \mathbf{V}_{XYZ} \qquad (2)$$

In a noise calibration measurement with no moved object in the sensitivity space below the sensor assembly, the appropriate noise weighting matrix $\boldsymbol{\omega}_{jk}$ has to be determined for all gradiometer channels j = A, B, C and in each of the 3 orthogonal fluxgate axes k = X, Y, Z.

3 Measurements and Results

3.1 Environmental magnetic noise

The city of Turin, especially the hospital area, is characterized by a dense traffic and street-car lines in a distance of about 200 m resulting in substantial environmental magnetic noise at frequencies < 5 Hz. First-order active noise cancellation (as described above) has been performed. Figure 2 shows the measurement of a cylindrical water phantom versus air reference with a large relative magnetic volume susceptibility of $\Delta\chi_{obj} = -9.396 \cdot 10^{-6}$ SI-units corresponding to a liver iron concentration of 5873 µg/g [10]. Although the slopes with and without active noise cancellation are relatively similar, measurements on objects and patients with only 10-20% of this signal strength would become extremely inaccurate and 1st-order linear fits would fail.

Extended environmental noise measurements including the moving patient bed, the powered ultrasound imager in a distance of 3m, and the active flat screen close to the fluxgate reference detector (= operational stand-by) did not result in significantly different coefficients of the noise weighting matrix $\boldsymbol{\omega}_{jk}$. In first order the reference signals were orthogonal and constant throughout 24 hours during the week (see Table 1).

Table 1: *Noise weighting coefficients for the 3-axis fluxgate reference signals with the biosusceptometer system in operational stand-by* ($\boldsymbol{\omega}_{AX} = \ldots = \boldsymbol{\omega}_{CY} = 0$).

	$\boldsymbol{\omega}_{AZ}$	$\boldsymbol{\omega}_{BZ}$	$\boldsymbol{\omega}_{CZ}$
mean	-125.6	65.8	-15.7
SD	2.1	1.2	1.5

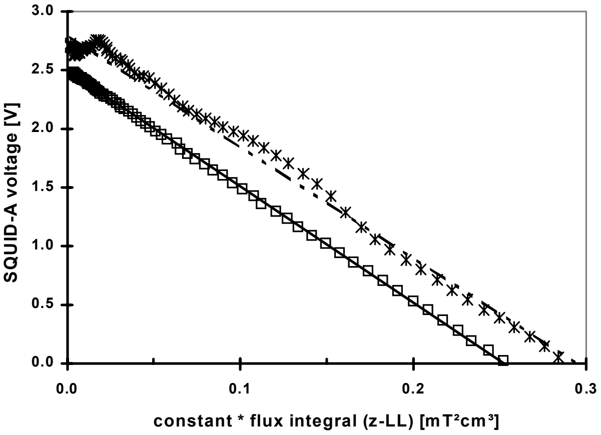

Figure 2: *Cylindrical water phantom (R=10 cm) measurement over a max. bed travel time of 15 s versus air reference with (squares) and without (stars) linear fluxgate noise subtraction in the vertical direction.*

3.2 System calibration measurements

System calibration can be performed by objects with well-known susceptibilities. The measurement of an infinite water half space (water tub of large diameter D >= 50 cm) is the most practical and precise method to determine the system calibration constant C [10]. The closest distance CD between the lowest gradiometer coil and the dewar tail was determined by x-ray imaging to be 1.6 cm. However, the simultaneous fit of both the calibration constant and the closest distance resulted in a slightly larger CD which is different for each SQUID gradiometer channel (see Fig. 3).

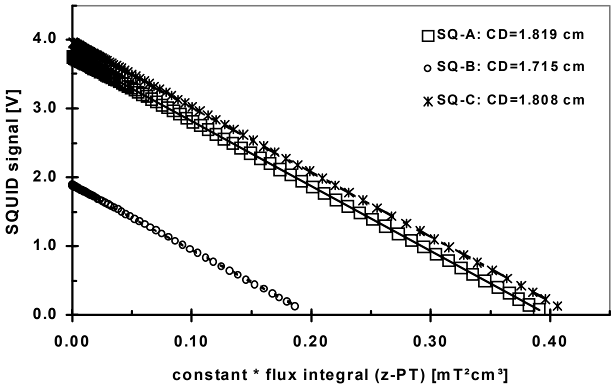

Figure 3: *Calibration of the Torino Biosusceptometer versus an infinite water half space with simultaneous fit of the closest distances CD of the lower gradiometer pick-up coils relative to the dewar tail* ($R^2 > 0.9999$).

With the closest distances from Fig. 3 we found the following calibration constants $C_A = 0.145 \pm 0.002$, $C_B = 0.46 \pm 0.02$, $C_C = 0.584 \pm 0.008$ [$VmT^{-2}cm^{-3}$] (see Eq. 1).

3.3 Preliminary phantom and patient measurements

First preliminary results in phantoms and in 4 patients measured with the Torino Biosusceptometer in comparison to the Hamburg reference system revealed similar system sensitivities and a reasonable agreement in the patient measurements:

On a cylindrical water phantom (25 L Nalgene® bottle) versus air reference, the system sensitivity was found to be 20, 28, and 14 µg/g (2 x SD) for the SQUID channels A, B, and C, respectively. Slightly worse results for the surface sensitive SQUID channels B and C were found from the measurement on a hollow cylindrical plexiglass phantom versus water reference. Also in patients the reproducibility was about the same size for SQUID channels A and C (± 40 and ± 10 µg/g), while according to its design, the planar SQUID gradiometer B seems to be extremely sensitive to surface effects like bad positioning of a patient.

However, at this state, there are some problems in the operation of the system which are mainly caused by shortcomings in the assessment of the patient's liver geometry by ultrasound, by difficulties with positioning, and by current poor quality calibration constants and system background contributions (Eq. 1).

In conclusion, after overcoming these initial problems and re-calibrating the system, we expect that the system can be operated in a clinical setting with no specific expert skills. Moreover, a standardized measurement protocol will allow routine liver and spleen iron quantitation. The new gradiometer configuration may allow future applications to other organs.

Acknowledgements

This work was supported by the Vigoni Program of the Deutscher Akademischer Austauschdienst (DAAD) and of the Conferenza dei Rettori delle Università Italiane (CRUI).

References

1. J.P. Kaltwasser, R. Gottschalk, K.P. Schalk, and W. Hartl, "Non-invasive quantitation of liver iron-overload by magnetic resonance imaging", *Brit. J. Haematol.* **74**, 360-363, 1990.
2. G.M. Brittenham, D.E. Farrell, J.W. Harris, E.S. Feldmann, E.H. Danish, W.A. Muir, J.H. Tripp, and E.M. Bellon, "Magnetic susceptibility measurement of human iron stores", *N. Eng. J. Med.* **307**, 1671-1675, 1982.
3. G.M. Brittenham, A.R. Cohen, C.E. McLaren M.B. Martin, P.M. Griffith, A.W. Nienhuis, N.S. Young, C.J. Allen, D.E. Farrell, and J.W. Harris, "Hepatic iron stores and plasma ferritin concentration in patients with sickle cell anemia and thalassemia major", *Am. J. Hematol.* **42**, 81-85, 1993.
4. R. Fischer, C.D. Tiemann, R. Engelhardt, P. Nielsen, M. Duerken, E.E. Gabbe, and G.E. Janka, "Assessment of iron stores in children with transfusion siderosis by biomagnetic liver susceptometry", Am. J. Hematol. **60**, 289-299, 1999.
5. D.E. Farrell, J.H. Tripp, P.E. Zanzucchi, J.W. Harris, G.M. Brittenham, and W.A. Muir, "Magnetic measurement of human iron stores", *IEEE Trans. Magn.* **16**, 818-823, 1980.
6. R. Engelhardt, K. Valett, and R. Fischer, "Printed circuit locator loop for x-y-positioning and z-distance measurements", in *Recent Advances in Biomagnetism*, T. Yoshimoto, M. Kotani, S. Kuriki, H. Karibe, and N. Nakasato, Eds. Sendai: Tohoku University Press, 1999, pp. 290-293.
7. D.N. Paulson, R.L. Fagaly, R.M. Toussaint, and R. Fischer, "Biomagnetic susceptometer with SQUID instrumentation", *IEEE Trans. Magn.* **27**, 3249-3252, 1991.
8. J.H. Tripp, "Physical concepts and mathematical models", in *Biomagnetism: an Interdisciplinary Approach*, S.J. Williamson, G.L. Romani, L. Kaufman, and I. Modena, Eds. Plenum, New York: Plenum Press, 1983, pp. 101-139.
9. S.E. Robinson, "Environmental noise cancellation for biomagnetic measurements", in *Advances in Biomagnetism*, S.J. Williamson, M. Hoke, G. Stroink, and M. Kotani, Eds. New York: Plenum Press, 1989, pp. 721-724.
10. R. Fischer, "Liver iron susceptometry", in *Magnetism in Medicine*, W. Andrä and H. Nowak, Eds. Berlin: Wiley VCH, 1998, pp. 286-301.